Al-Azhar Bulletin of Science

Volume 27 | Issue 1 Article 6

6-1-2016

Section: Mathematics, Statistics, Computer Science, Physics and Astronomy

LONGITUDINAL COUPLING IMPEDANCE FOR PARTICLE BEAMS OF PARABOLIC TRANSVERSE CHARGE ISTRIBUTION MOVING IN A RESISTIVE CULINDRICAL BEAM-PIPE OF FINITE WALL THICKENS

AHMED AL-KHATEEB
Yarmouk University, College of Science, Department of Physics, Kingdom of Jordan

NOUF AL-SALEEM
Department of physics, College of Education in Jubail, University of Dammam, Kingdom of Saudi Arabia

How to Cite This Article

AL-KHATEEB, AHMED and AL-SALEEM, NOUF (2016) "LONGITUDINAL COUPLING IMPEDANCE FOR PARTICLE BEAMS OF PARABOLIC TRANSVERSE CHARGE ISTRIBUTION MOVING IN A RESISTIVE CULINDRICAL BEAM-PIPE OF FINITE WALL THICKENS," *Al-Azhar Bulletin of Science*: Vol. 27: Iss. 1, Article 6.
DOI: https://doi.org/10.21608/absb.2016.60511

Al Azhar Buletin of Science Vol.(27) No.1, June, 11-18, 2016.

LONGITUDINAL COUPLING IMPEDANCE FOR PARTICLE BEAMS OF PARABOLIC TRANSVERSE CHARGE DISTRIBUTION MOVING IN A RESISTIVE CULINDRICAL BEAM-PIPE OF FINITE WALL THICKENS

AHMED M. AL-AL-KHATEEB[1] AND NOUF K. AL-SALEEM[2]

[1]*Yarmouk University, College of Science, Department of Physics, Kingdom of Jordan*
[2]*Department of physics, College of Education in Jubail, University of Dammam, Kingdom of Saudi Arabia*

ABSTRACT

The longitudinal coupling impedance for particle beams of parabolic transverse charge distribution moving in a resistive cylindrical beam-pipe of finite wall thicken studied theoretically. The particle beam is moving at constant speed down a resistive cylindrical pipe of fintie wall thickness. The wave equations for the lectromagnetic fields induced by the beam motion inside the cylindrical pipe have been derived and solved. The space charge and the wall impedances have been obtained analyticaaly and then analyzed numberically for diferent beam energies, diferent wall conductivities and diferent wave mode frequencies. The real part for the wall impedance is found to be a positive resistance while the imaginary part is a positive reacetance (inductive). At low beam energies we observed no differences between the impedances of quadratic and uniform beams. At high beam energies and for all wave mode frequencies, differences between the two impedance are observed frow all thickness bellow the skin penetration depth δs. The impedance converges for large wall thicknetowared a small value of the order of the sufface impedance of a thick conducting wall.

Key Words : *Power Transmission, Waveguides*

I. INTRODUCTION

In the design phase of an accelerator it is desired to reduce the coupling impedance of the beam to its environment in order to prevent the beam instabilities. The longitudinal coupling impedance includes the space-charge and the resistive-wall parts. It is an important physical quantity in liner and circular accelerators as well as in storage rings for bettter understanding and for modeling to the longitudinal dynamics of charged particle beams and their instabilities. A beam of charged particles can exacite electromagnetic fields in its environment and periodice excitation can occur depending on the coupling of the beam to its environment at a particular frequency.

II. IMPEDANCE

The term impedance was first used by Heaviside in 19th century to escribe the complex ratio of the voltage to the current $Z(\omega)= V(\omega)/I(\omega)$ in alternating alternating current circuits (AC circuits) consisting of a resistor R, inductors L and capacitors C [1,2]. The impedance $Z(\omega)$ is a complex quantity which can be written as $Z(\omega) = R(\omega) – i\chi(\omega)$ in physical conventions or as $Z(\omega) = R(\omega) = j\chi(\omega)$ in engineering conventions, where $– i = j$. The real part o impedance R is the resistance of the circuit, and its imaginary part χ is the reactance of the circuit. In direct current (DC) circuits, the impedance corresponds to a pure resistance.

Schelkunoff was the first one who recognized that the impedance concept could be extended to electromagnetic field in systematic way. He noted that impedance can be regarded as a characteristic of the field type as well as of the medium [3]. The concept of impedance can be regarded as an important link between field theory and circuit theory [2, 4]. The effects of beam interaction with a vacuum chamber (or a beam-pipe) are treated in the frequency domain in terms of coupling impedance's: longitudinal impedance, $Z\|$ and transverse impedance $Z\perp$. In accelerator physics applications, the concepts of longitudinal and transverse beam effects (excited fields or impedance's) become of importance [5–9]. An impedance imaginary part is usually classified as inductive or capacitive according to its sign. In engineering conventions, a positive imaginary part is called inductive and a negative imaginary part is called capacitive. The longitudinal impedance $Z\|$ and the

transverse impedance Z⊥ are usually introduced and are measured, respectively, in Ω and Ω/meter [10, 11]. The coupling impedance includes the a space-charge and a resistive-wall impedance's it is written as follows [5, 10,12],

$$Z^{(total)}(\omega) = (\omega)Z^{(sc)}(\omega) + Z^{(rw)}(\omega) \quad (1)$$

Where $Z^{(sc)}(\omega)$ is the space charge impedance (corresponds to the case when the beam pipe wall is perfectly conducting), and $Z^{(rw)}(\omega)$ is the resistive wall impedance (when the beam pipe wall is resistive and has a finite wall conductivity).

III. SPACE-CHARGE AND RESISTIVE WALL IMPEDANCES

Space-charge and resistive-wall impedance's are important topics in liner and circular accelerators as well as in storage rings and particle beam physics. When the particles charge are accelerated, guided and confined by external electromagnetic fields. It is mean the not effect of the Coulomb interactions in a multi-particle system. Space-charge fields are the self electromagnetic fields a moving particle beam generates in a given beam-pipe structure. Due to the strong electromagnetic fields that follow the beam, it is possible for it to interact with any impedance in the walls of the beam pipe. This may be in the from of a resistive wall impedance or an inductive or capacitive impedance according to its sign.

For a perfectly conducting wall with large S the $Z^{(rw)} \rightarrow 0$. The impedance in the limit of a perfectly conducting wall becomes the so called the space-charge impedance $Z^{(sc)}(\omega)$. The resistive wall impedance $Z^{(rw)}(\omega)$ which accounts for the wall effects has been defined as follows:

$$Z^{(rw)}(\omega) = Z^{(total)}(\omega) - (\omega)Z^{(sc)}(\omega) \quad (2)$$

IV. THEORETICAL MODEL AND METHODOLOGY

The main problem is calculate the longitudinal coupling impedance for particle beams of parabolic transverse charge distribution moving in a resistive cylindrical beam-pipe of finite wall thickens. The coupling Impedance is definition can be derived as a volume integral over the transverse distribution of the beam [11],

(3)

where $Z(\omega)$ is impedance, and $I_b(\omega)$ is current of the beam in frequency domain. In order to calculate the coupling impedance we need the component of the electric field $E(r, \omega)$ and the - current density $jb(r, \omega)$.

From Faradays and Amperes laws in a linear conducting medium, we have the following wave equations for the magnetic induction B and electric field E [11, 14]:

$$\left[\vec{\nabla}^2 - \mu_0\varepsilon_0 \frac{\partial}{\partial t^2} - \mu_0 S \frac{\partial}{\partial t}\right]\vec{B}(\vec{r},t) - \mu_0\vec{\nabla} \times \vec{j}_b(\vec{r},t) \quad (4)$$

$$\left[\vec{\nabla}^2 - \mu_0\varepsilon_0 \frac{\partial}{\partial t^2} - \mu_0 S \frac{\partial}{\partial t}\right]\vec{B}(\vec{r},t) - \mu_0 \frac{\partial}{\partial t}\vec{j}_b(\vec{r},t)\frac{1}{\varepsilon_0}\vec{\nabla}\rho b(\vec{r},t) \quad (5)$$

Where ε_0 and μ_0 respectively, the free space permeability and S is the conductivity of medium under consideration. Here ρb and $\bar{j}b$ are the beam charge and current densities, respectively. We consider a beam of particles of radius a with an axially symmetric transverse charge distribution $\sigma(r)$ which move at a constant speed along the axis of a cylindrical beam-pipe of radius b. With a longitudinal beam velocity such that $-v = \beta c\hat{z}$ along the z axis, we have the following beam charge and current densities:

$$\rho b(r, z, t) = \sigma(r)\delta(z - \beta ct) , \quad (6)$$

$$jb(r, t) = \beta c \rho b (-r, t)\hat{z}. \quad (7)$$

Here β is the relativistic factor and c is the speed of light in vacuum. For a uniformly charged disk of total charge Q

$$Q = 2\pi\sigma(r) r\, dr . \quad (8)$$

The Fourier time-transformed beam charge and current densities are,

$$\rho b (r, z, \omega) = e\, i\, kz\, z . \quad (9)$$

$$\beta c\, jb(r, z, \omega) = \sigma(r)\, e^{ikz}, ikz\, z . \quad (10)$$

For a uniformly charged thin disk of radius charge Q, the surface charge density distribution in the transverse direction is

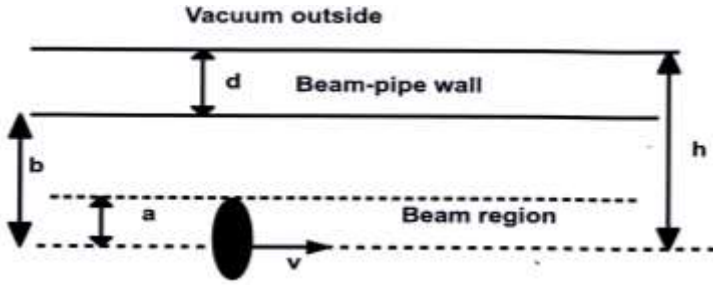

FIG. 1: Pipe geometry

(11)

Where kz stands for number in the direction of beam propagation and ω = kzβc has been introduced. For the axial symmetric beam of equations (36) and (7), only transverse magnetic (TM) modes couple to the propagating beam. The non-vanishing electro-magnetic field components are Ez, Er and B_θ. the electromagnetic field components E_θ and Br vanish identically because of the axial symmetry of the beam. Assuming a normal mode solution for electric Ez such that $E(r, z, \omega) = e\ (r, \omega)\ e^{ikz}$ and by making use of ρb (r, z, ω) and jb(r, z, ω) in equations (9) and (10), we obtain the following equations the longitudinal electric field component in each region of Fig 1 :

$$\frac{d^2}{dr^2} + \frac{1}{r}\frac{1d}{r\,dr} - \frac{k^2}{\gamma_0^2}\vec{e}_z^{(1)}(r,w) = \frac{ik_z c}{\beta \in_0 c\gamma_0^2}\frac{2Q}{\pi a^2},\ 0 \le r \le a \quad (12)$$

$$\left[\frac{d^2}{dr^2} + \frac{1}{r}\frac{1d}{r\,dr} - \frac{k^2}{\gamma_0^2}\right]\vec{e}_z^{(2)}(r,w) = 0, \qquad a \le r \le b. \quad (13)$$

$$\left[\frac{d^2}{dr^2} + \frac{1}{r}\frac{1d}{r\,dr} - \frac{k^2}{\gamma_0^2}\right]\vec{e}_z^{(3)}(r,w) = 0, \qquad b \le r \le h = b + d. \quad (14)$$

$$\left[\frac{d^2}{dr^2} + \frac{1}{r}\frac{1d}{r\,dr} - \frac{k^2}{\gamma_0^2}\right]\vec{e}_z^{(4)}(r,w) = 0, \qquad h \le r \le \infty \quad (15)$$

Here γ_0^{-2} has been introduced as follows:

$$\gamma_0^{-2} = 1 - \beta^2, \frac{1}{\gamma_c^2} = \frac{1}{\gamma_0^2} - \frac{iw\mu_0 S}{k_z^2} \quad (16)$$

The azimuthal magnetic field component hθ(r,z,ω) needed for matching the solutions at the different interfaces involved in the problem is obtained form Maxwell's curl equations as follows:

$$b_\theta = \frac{-i\gamma_c^2}{k_z}\frac{\beta}{c}\left(1+\frac{S}{\in_0 w}\right)\frac{\partial e_z}{\partial r} \tag{17}$$

Where γ in equation (17) stands for γc in vacuum, for γc in the beam-pipe wall. The general solution for the z-component of the electric field is,

$$e_z\begin{cases} A_1 I_0(\sigma_0 r) - i\dfrac{2Q}{\pi a^2 \in_0 k_z \beta c}\left(1-\dfrac{r^2}{a^2}-\dfrac{4}{\sigma_0^2 a^2}\right) & r \le a \\ A_1 I_0(\sigma_0 r) + A_3 K_0(\sigma_0 r) & a \le r \le b \\ A_1 I_0(\sigma_0 r) + A_3 K_0(\sigma_c r) & b \le r \le h \\ A_1 I_0(\sigma_0 r) & h \le r < \infty \end{cases} \tag{18}$$

Where $\sigma_0 = \frac{k_2}{\gamma_0} = \frac{w}{\beta_c \gamma_0}, \sigma_c = \frac{k_2}{\gamma_c}, I_0$ and k_0 are modified Bessel function of first and second kind respectively. The corresponding azimuthal magnetic field is,

$$b_\theta(r,w) = \begin{cases} -i\dfrac{\gamma_0^2}{k_z}\dfrac{\beta}{c}\left[A_1\sigma_0 I_1(\sigma_0 r) + i\alpha\dfrac{2}{a}\right] & 0 < r < a \\ -i\dfrac{\gamma_0^2}{k_z}\dfrac{\beta}{c}\left[A_1\sigma_0 I_1(\sigma_0 r) - A_3\sigma_0 K_1(\sigma_0 r)\right] & 0 < r < b \\ -i\dfrac{\gamma_0^2}{k_z}\dfrac{\beta}{c}\left(1+i\dfrac{S}{w\in_0}\right)\left[A_1\sigma_0 I_1(\sigma_0 r) - A_3\sigma_c K_1(\sigma_c r)\right] & b < r < h \\ -i\dfrac{\gamma_0^2}{k_z}\dfrac{\beta}{c}\left[A_3\sigma_c K_1(\sigma_c r)\right] & h < r < \infty \end{cases} \tag{19}$$

Applying the boundary conditions on the tangential field components e_z and h_θ at all interfaces at r = a, r = b, r = h we obtain the following closed system of algebraic equations for the integration constants:

$$A_1 I_0(\sigma_0 a) + ia\frac{4}{\sigma_0^2 a^2} = A_1 I_0(\sigma_0 a) + A_3 K_0(\sigma_0 a), \text{continuity of } E_z \text{ at } r = a \tag{20}$$

$$A_1 I_1(\sigma_0 a) + ia\frac{2}{\sigma_0 a} = A_2 I_1(\sigma_0 a) + A_3 K_1(\sigma_c a), \text{continuity of } E_z \text{ at } r = a \tag{21}$$

$$A_2 I_0(\sigma_0 b) + A_3 K_0(\sigma_0 b) = A_4 I_0(\sigma_c b) + A_5 K_0(\sigma_c b), \text{continuity of } E_z \text{ at } r = b \tag{22}$$

$$\eta_c[A_2 I_0(\sigma_0 b) - A_3 K_1(\sigma_0 b) = A_4 I_0(\sigma_c b) + A_5 K_1(\sigma_c b), \text{continuity of } B_\theta \text{ at } r = b \tag{23}$$

$$A_4 I_0(\sigma_0 h) + A_5 K_0(\sigma_c h) = A_6 K_0(\sigma_0 h), \text{continuity of } B_\theta \text{ at } r = h \tag{24}$$

$$A_4 I_1(\sigma_c h) + A_5 K_0(\sigma_c h) = \eta_c A_6 K_1(\sigma_0 h), \text{continuity of } B_\theta \text{ at } r = h \tag{25}$$

Where the parameters η_c and a are defined as follows

$$\eta_c = \frac{\gamma_0}{\gamma_c(1+i\frac{\mu_0 c^2 S}{w})} = \frac{\gamma_0 w \in_0}{i\gamma_c(S - iw\in_0)}, \qquad a = \frac{2Q}{\pi a^2 w \in_0}$$

$$A_1 = 2i\alpha I_1(\sigma_1 a)\left[\frac{I_0(\sigma_1 a) + RK_0(\sigma_1 a)}{I_1(\sigma_1 a) - RK_1(\sigma_1 a)} - \frac{2}{(\sigma_1 a)}\right]\left[\frac{K_1(\sigma_1 a)}{I_1(\sigma_1 a)} - \frac{1}{R}\right], \tag{26}$$

$$A_2 = \frac{I_0(\sigma_1 a)}{I_1(\sigma_0 a) - RK_1(\sigma_0 a)} - A_1 += \frac{ia\frac{2}{(\sigma_0 a)}}{I_1(\sigma_0 a) - RK_1(\sigma_0 a)} \tag{27}$$

$$A_3 = RA_2, \tag{28}$$

$$A_4 = \frac{I_0(\sigma_0 b) + RK_0(\sigma_1 b)}{I_0(\sigma_c b) - FK_0(\sigma_c b)} \tag{29}$$

$$A_5 = RA_4, \tag{30}$$

$$A_6 = \frac{I_0(\sigma_c h)}{K_0(\sigma_0 h)}A_4 + \frac{K_0(\sigma_c h)}{K_0(\sigma_0 h)}A_5, \tag{31}$$

$$R = \frac{\eta_c I_1(\sigma_0 b) - GI_0(\sigma_0 b)}{\eta_c K_1(\sigma_0 b) - GK_0(\sigma_0 b)} \tag{32}$$

$$G = \frac{I_1(\sigma_c b) - FK_1(\sigma_c b)}{I_0(\sigma_c b) + FK_0(\sigma_c b)} \tag{33}$$

$$F = \frac{I_1(\sigma_0 h)K_0(\sigma_0 h) + \eta_1 K_1(\sigma_0 h)I_0(\sigma_c h)}{K_1(\sigma_0 h)K_0(\sigma_0 h) - \eta_c K_1(\sigma_0 h)K_0(\sigma_c h)} \tag{34}$$

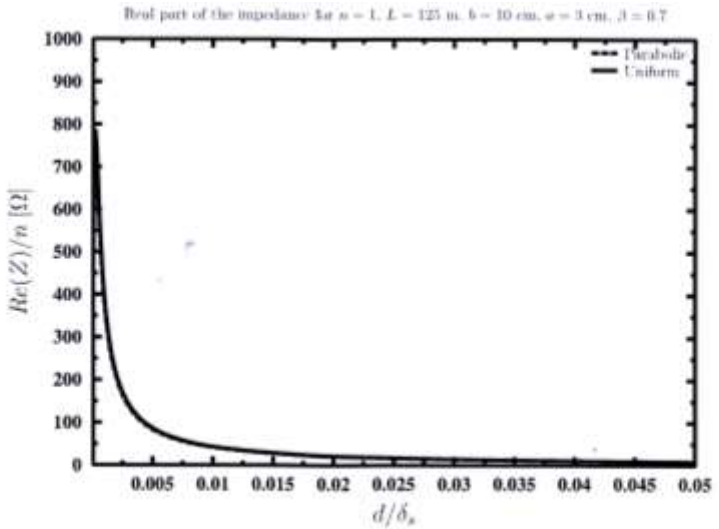

FIG. 2: Comparison between the real parts of the resistive wall impedance for parabolic and uniform beams for the lowest harmonic n = 1 at beam speed 0.7.

V. THE LONGITUDINAL COUPLING IMPEDANCE

$$
\begin{aligned}
Z_{\parallel}(w) &= i\alpha \frac{8L}{Q\sigma_0^2 a^2}\left[B_1 I_2(\sigma_0 a) + \frac{1}{2} - \frac{\sigma_0^2 a^2}{12} \right] \\
&= i \frac{2Q}{\pi a^2 w \in_0} \frac{8L}{Q\sigma_0^2 a^2}\left[B_1 I_2(\sigma_0 a) + \frac{1}{2} - \frac{\sigma_0^2 a^2}{12} \right] \\
&= i \frac{4L}{\pi a^2 w \in_0} \frac{4}{\sigma_0^2 a^2}\left[B_1 I_2(\sigma_0 a) + \frac{1}{2} - \frac{\sigma_0^2 a^2}{12} \right] \\
&= i \frac{nZ_0}{2\beta\gamma_0^2} \frac{16}{\sigma_0^4 a^4}\left[4B_1 I_2(\sigma_0 a) + 2 - \frac{\sigma_0^2 a^2}{3} \right] \\
Z_{\parallel}(w) &= in\chi_0 \frac{16}{\sigma_0^4 a^4}\left[B_1 I_2(\sigma_0 a) + 2 - \frac{\sigma_0^2 a^2}{3} \right]
\end{aligned}
\tag{35}
$$

Where g_f is an equivalent geometry factor which accounts for the beam properties and beam-pipegennetry and conductivity. Here we have $I_2(x) = I_0(x) - \sigma_0 = \frac{2h}{x}$ and $B_1 = \frac{A_1}{i\alpha}$ such that,

$$
B_1 = 2I_1(\sigma_0 a)\left[\frac{I_0(\sigma_0 a) + RK_0(\sigma_0 a)}{I_1(\sigma_0 a) - RK_1(\sigma_0 a)} - \frac{2}{\sigma_0 a} \right]\left[\frac{K_1(\sigma_0 a)}{I_1(\sigma_0 a)} - \frac{1}{R} \right] \tag{36}
$$

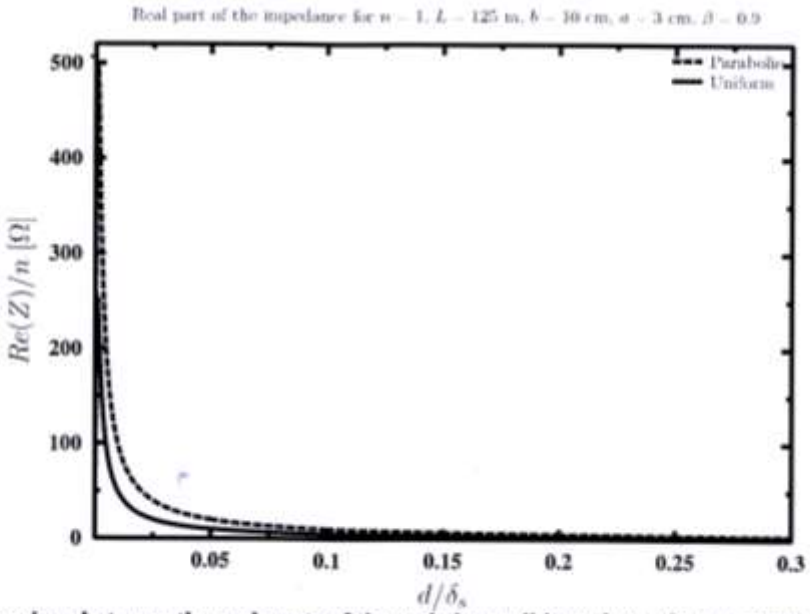

FIG. 3: Comparison between the real parts of the resistive wall impedance for parabolic and uniform beams for the lowest harmonic n = 1 at beam speed 0.9.

VI. THE CASE OF A GOOD CONDUCTING WALL

For a good conductors wall with large S or σ_c, we have large values σc. The argument σcb or σch of Bessel function is also large. For large argument, we have,

$$I_m(x) \to \frac{1}{\sqrt{2\pi x}} e^x,\ K_m(x) \to \sqrt{\frac{\pi}{2x}} e^{-x} \tag{37}$$

The parameter F becomes,

$$F = \frac{I_0(\sigma_c h)}{K_1(\sigma_c h)} \left[\frac{K_0(\sigma_0 h) + \eta_c K_1(\sigma_0 h)}{K_0(\sigma_0 h) - \eta_c K_1(\sigma_0 h)} \right] \tag{38}$$

We also have,

$$\frac{K_m(x)}{I_m(x)} = \sqrt{\frac{\pi}{2x}} \sqrt{2\pi x} \frac{e^{-x}}{e^x} \pi e^{-2x} \tag{39}$$

$$F \approx \frac{1}{\pi} e^{2\sigma_c h} \left[\frac{K_0(\sigma_0 h) + \eta_c K_1(\sigma_0 h)}{K_0(\sigma_0 h) - \eta_c K_1(\sigma_0 h)} \right] \tag{40}$$

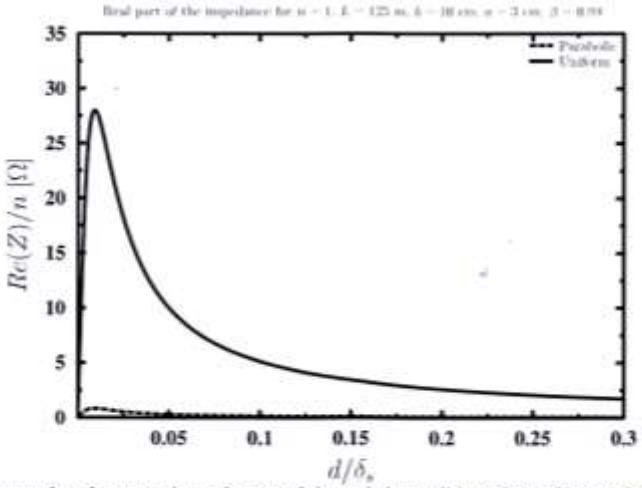

FIG. 4: Comparison between the real parts of the resistive wall impedance for parabolic and uniform beams for the lowest harmonic number n = 1 at beam speed 0.99.

The parameter G can be written as follows,

$$G = \left[\frac{K_0(\sigma_0 h) - \eta_c \coth(\sigma_c d)\ K_1(\sigma_0 d)}{\eta_c K_1(\sigma_0 h) - \coth(\sigma_c d)\ K_0(\sigma_0 d)} \right] \tag{41}$$

For a perfectly conducting wall we have ηc → 0 and G → –1 , therefore that parameter R becomes R → – $I_0(\sigma 0b)/K_0(\sigma 0b)$. The impedance in the limit of a perfectly conducting wall (sc) (rw) becomes the so called the space-charge impedance Z(ω). The resistive wall impedance Z (w) which accounts for the wall effects has been defined as follows:

$$Z_{\parallel}^{(rw)}(w) = Z_{\parallel}(w) - Z_{\parallel}^{(sc)} \tag{42}$$

WII. NUMERICAL EXAMPLE

We summarize our numerical results as follows,

1. Figure 2 shows the real part of the impedance normalized to the harmonic number in Ω versus wall thickness normalized to the skin depth δs. For n = 1 and β =0.7 we observe no difference between the impedance of parabolic and uniform beams.

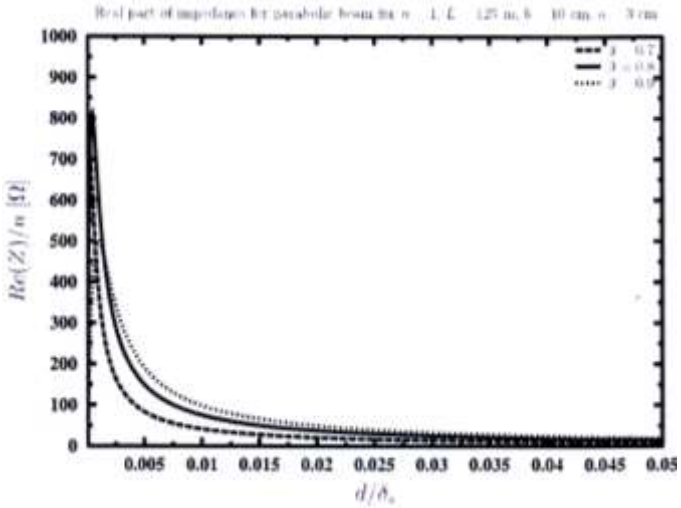

Fig. 5: Comparison between the real parts of the resistive wall impedance for the parabolic beam for the harmonic number n = 1 at different beam speeds.

2. Figure 3 shows the real part of the impedance normalized to the harmonic number in Ω versus wall thickness normalized to the skin depth δs. For n = 1 and β =0.9 we observe a difference between the impedance of parabolic and uniform beams for a wall thickness approximately bellow 0.05 δs. But Fig. 4 we observe a big difference between the curves of the impedances for parabolic and uniform beams in the high energy limit

3. Figure 5 and Figure 6 shows a real part of impedance normalized to the harmonic number in Ω versus wall thickness normalized to the skin depth δs. All figures have the same harmonic number n = 1 but different resolutions along the x axis. We observe from Figure 5 that the value of the impedance will not go zero for large wall thicknesses d, as can be seen from and Figures 6.

For large values of wall thicknesses d, the impedance converges toward a small value of the order of the surface impedance of a thick conducting wall. The surface impedance is the impedance of a conducting medium of conductivity σw to the propagation of a plane electromagnetic wave. The following expression for the surface impedance of a thick wall in engineering conventions is found in many textbooks [2, 4, 10],

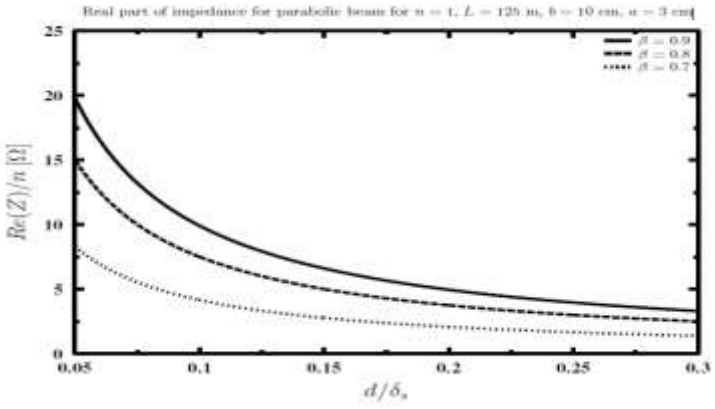

FIG 6: Comparison between the real parts of the resistive wall impedance for the parabolic beam for the harmonic number n = 1 at different beam speeds.

4. The curves of Figure 7 shows the negative imaginary part of the resistive wall impedance versus normalized wall thickness for three different energies. In engineering conventions such that −i = j, the imaginary part is positive and therefore, it is inductive in nature. For large wall thicknesses d, it converges asymptotically toward the surface impedance of the wall and will not go to zero.

VIII. CONCLUSIONS

The longitudinal coupling impedance of a particle beam of parabolic (quadratic) transverse charge distribution has been presented in this thesis work, theoretically and numerically. The beam is moving at constant speed down a resistive cylindrical beam-pipe of finite wall thickness. The space-charge and resistive-wall impedance's have been obtained analytically and then analyzed numerically for different beam energies, different wall conductivities and different wave mode (harmonic) frequencies. The coupling impedance is used in beam dynamics and in the analysis of beam instabilities. We now summarize the main results and conclusions of the analytical and numerical calculations as follows:

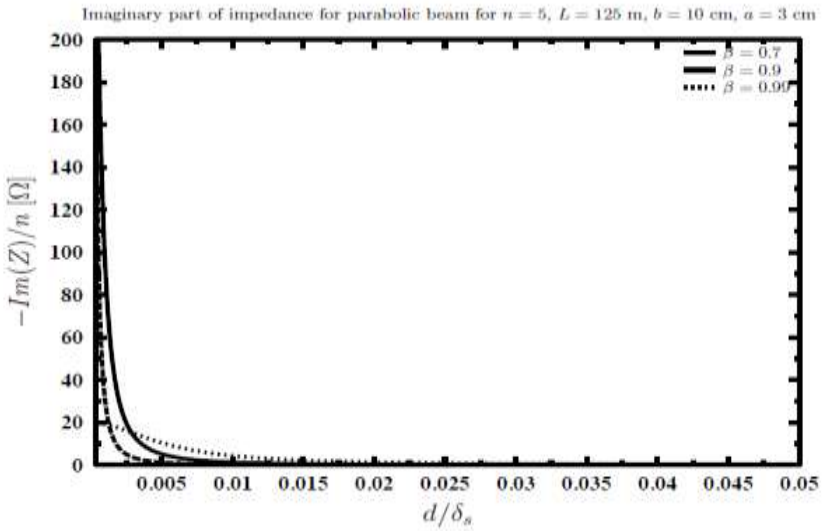

FIG. 7: Comparison between the imaginary parts of the resistive wall impedance at different beam speeds for the harmonic number n = 5.

at low beam energies, no obvious difference is observed between the impedance of parabolic and uniform beams (see Fig. 2), by raising the beam energy, we observe a difference between the impedance of parabolic and uniform beams for thickness much bellow the skin penetration depth, namely, for $d \leq 0.05\ \delta s$ (see Fig4), for the harmonic number n = 1, for example, we observe that the impedance of the parabolic beam for different beam energies converges toward a small value for large wall thicknesses (see Fig 6 . This small value is of the order of magnitude of the surface impedance of the wall Zs, in engineering convention −i = j, the imaginary part of the resistive wall is positive which means that it is inductive in nurture (see Fig 7).

IX. REFERENCES

[1] A. A. Oliner, IEEE Trans. Microwave Theory Tech. 32, p.1022 (1985).

[2] D. M. Pozar, Microwave Engineering, Addison–Wesley, 1990.

[3] A. Schelkunoff, Electromagnetic Waves, Van Nostrand, New York, 1943.

[4] R. E. Collin, Field Theory of Guided Waves, McGraw- Hill, New York, 1960.

[5] R.L. Gluckstern, Analytical Methods for Calculating Coupling Impedances, CERN report 2000-011, p.9 (2000).

[6] F. Zimmermann and K. Oide, Phys. Rev. STAB 7, p. 044201 (2004).

[7] B. Zotter, CERN report CERN-AB-043.

[8] E. M´etral, CERN report CERN-AB-084.

[9] R. L. Gluckstern and B. Zotter, Phys. Rev. STAB 4, 024402 (2001).

[10] Alexander Wu Chao, Physics of Collective Beam Instability in High Energy Accelerators, John Wiley and Sons, 1993.

[11] B. W. Zotter and S. A. Kheifets, Impedances and Wakes in High-Energy Accelerators, World Scientific, Singapore,1998.

[12] M. Reiser, Theory and Design of charged Particle Beams, Wiley, New York,1994.

[13] D. A. Edwards and M. J. Syphers, An Introduction to the Physics High Energy Accelerators, John Wiley, 1993.

[14] J. D. Jackson, Classical Electrodynamics, John Wiley, 1975.

[15] R. E. Collin, Field Theory of Guided Waves, McGraw- Hill, New